

Bacterial cellulose–silica organic–inorganic hybrids

H. S. Barud · R. M. N. Assunção · M. A. U. Martines · J. Dexpert-Ghys ·
R. F. C. Marques · Y. Messaddeq · S. J. L. Ribeiro

Received: 25 August 2007 / Accepted: 6 December 2007 / Published online: 25 December 2007
© Springer Science+Business Media, LLC 2007

Abstract Bacterial cellulose (BC) hydrated membranes present nanometric reticulated structure that can be used as a template in the preparation of new organic–inorganic hybrids. BC–silica hybrids were prepared from BC membranes and tetraethoxysilane, (TEOS) at neutral pH conditions at room temperature. Macroscopically homogeneous membranes were obtained containing up to 66 wt.% of silica spheres, 20–30 nm diameter. Scanning electron micrographs clearly show the silica spheres attached to cellulose microfibrils. By removing the cellulose, the silica spheres can be easily recovered. The new hybrids are stable up to 300 °C and display a broad emission band under UV excitation assigned to oxygen-related defects at the silica particles surface. Emission color can be tuned by changing the excitation wavelength.

Keywords Bacterial cellulose · Silica · Organic–inorganic hybrids

H. S. Barud · R. M. N. Assunção · R. F. C. Marques ·
Y. Messaddeq · S. J. L. Ribeiro (✉)
Institute of Chemistry, São Paulo State University-UNESP,
CP 355, Araraquara, SP 14801-970, Brazil
e-mail: sidney@iq.unesp.br

R. M. N. Assunção
Institute of Chemistry, Federal University of Uberlândia,
CP 593, Uberlândia, MG 38400-902, Brazil

M. A. U. Martines
Department of Chemistry and Physics, FEIS-São Paulo State
University-UNESP, Ilha Solteira, SP 15385-000, Brazil

J. Dexpert-Ghys · R. F. C. Marques
Centre d'Elaboration de Matériaux et d'Etudes Structurales,
UPR N°8011 – Université Toulouse III, B.P. 94347,
29 rue Jeanne Marvig, 31055 Toulouse Cedex, France

1 Introduction

The observation of tunable room temperature emission from porous silicon layers in 1990 [1] triggered the interest in light emitting silicon-based materials. In fact the development of optically efficient silicon-compatible materials, allowing complete integration of optical and electronic devices will impact for sure displays, communications, computers and related technologies [2, 3]. In parallel, organic–inorganic (OI) composites gather together typical advantages of organic polymers like flexibility, low density, toughness, and formability, with the ones displayed by typical inorganic materials like hardness, chemical resistance, strength, optical properties among others [4]. Considerable efforts have then been focused in exploring the rich chemistry of silicon in the preparation of stable and efficient white light photoluminescent organic–inorganic hybrids lacking metal activator ions [5]. The outgrowth of full-color displays cheaper and less aggressive to the global environment and that could replace the metal emissive centers currently used with substantial advantages, is one of the main challenging tasks for the next generation of flat-panel displays systems and lighting technologies.

Considering the polymeric counterpart in OI composites renewed interest is found on cellulose. Cellulose is the most abundant natural biopolymer on earth. It is therefore biodegradable and produced by renewable resources like plants and bacteria [6, 7].

Cellulose produced by Gram-negative, acetic acid bacteria *Gluconacetobacter xylinus* displays several unique properties when compared to plant cellulose. It is produced as highly hydrated membranes (up to 99% water), free of lignin and hemicelluloses and displaying higher molecular weight and higher crystallinity, in a nanometric reticulated structure. Applications range from paper and textile industry

to cosmetics and medicine [8–11]. In fact one of the most promising areas of bacterial cellulose (BC) application as biomaterials is the utilization as a temporary skin substitute in the therapy of difficult wounds, burns and ulcers [8]. The possibility of incorporating silver nanoparticles extend the biomedical applications [12].

Cellulose–silica composite materials have been considered in the literature. Hydroxypropylcellulose–siloxane composites have been prepared in [13] from hydroxypropylcellulose and tetraethoxysilane (TEOS) precursors. Acid catalysis was employed in the hydrolysis/condensation of TEOS and an increase in the dynamic modulus is observed with the increase in silica content (up to 25 wt.%) as compared with the one obtained for pure cellulose. Interaction between the two phases was found to occur mainly through hydrogen bonds. Acetylcellulose–silica composites have been considered in [14]. The structure was found to be composed of micrometer sized particles rich in silica and a matrix rich in acetylcellulose.

Cellulose structure is also used as templates in mineralization process. Mesoporous silica could be obtained from cellulose nanorod nematic suspensions [15]. Authors claim that it could be a cost-effective, environmental benign route applied in the template synthesis of mesoporous materials.

Trying to mimic nature in the silica mineralization process, BC–silica hybrids were studied in [16]. In some plants like rice, silica biomineralization occurs through the deposition of amorphous silica on a polysaccharide matrix [17]. TEOS acid catalysed hydrolysis was employed and nanoscale silica was observed embedded in cellulose micro-fibrils [16]. As a consequence an increase in the modulus of elasticity and tensile strength was observed.

By using eucalyptus bleached kraft pulp as cellulose source and heteropoly acids as catalysts in the TEOS hydrolysis/condensation cellulose–silica hybrids were also prepared in [18]. Under the catalysis conditions used silica was observed to be present in the form of a thin film deposited on cellulose fibers. Up to 60 wt.% silica could be incorporated diminishing hydrophilic properties and improving thermal stability.

In this work BC–silica hybrids were prepared from BC hydrogels and TEOS under neutral pH conditions. Almost nanometer sized silica spheres were obtained attached to cellulose microfibrils. Thermal and structural characteristics are presented. A preliminary luminescence study shows that new broad band tunable emission luminescent materials are obtained.

2 Experimental

Tetraethoxysilane (TEOS) was submitted to hydrolysis/condensation process in situ on the cellulose microfibrils.

BC hydrogel membranes ($3 \times 6 \times 0.5$ cm) were soaked in 3 mL TEOS/Ethanol solutions with TEOS:ethanol relative quantities (in mL) 0.9:2.1, 1.4:1.6, 1.8:1.2, 2.2:0.8. After 24 h samples were dried for 12 h at 50 °C.

Scanning electron microscopy (SEM) images were obtained in a Field Emission Scanning Electron Microscopy JEOL JMF-6700F model. Samples were covered with a 1 nm thick gold layer on copper supports.

Infrared absorption spectra were obtained from 4,500 to 400 cm^{-1} by using KBr pellets in a FTIR Spectrum 2000 Perkin-Elmer spectrometer.

X-ray diffraction patterns (XRD) were obtained in a Siemens Kristalloflex diffractometer using nickel filtered Cu K_α radiation in the 2θ angle range from 4 to 70°.

Thermogravimetric analyses (TGA curves) were obtained in a SDT 2960 from TA-Instruments. Samples were heated in open α -alumina pans from 40 to 500 °C under nitrogen atmosphere, 70 mL min^{-1} , at heating rate of 10 °C min^{-1} .

Room temperature emission spectra were obtained in SPEX Fluorolog F212I spectrofluorimeter equipped with a 450 W continuous Xe lamp as excitation source and a Hamamatsu R928 photomultiplier in the detection set-up.

3 Results and discussion

Macroscopically homogeneous, around 500 μm thick, BC–silica composite membranes were obtained transparent to milky, depending on the silica content. Under the experimental conditions used the final silica content, as obtained from TGA analysis shown hereafter, were (in weight) 28, 49, 62 and 66%.

Figure 1 shows representative SEM micrographs of BC and the BC–silica composite containing 66wt.% silica. The nanofibers network of BC membranes and silica spherical particles, 20–30 nm diameter, embedded in the fibers structure are clearly observed. The three-dimensional support of the high surface area of BC allows nanoparticles formation. Hydrolysis and condensation of TEOS embedded in the microfibrils interspace lead to the well dispersed nanosized silica spherical particles.

This 66% silica sample was treated at 400 °C in air to remove the cellulose template and the residue was analyzed by Transmission Electron Microscopy (TEM). Figure 2 shows the spherical silica particles, 20–30 nm diameter, so obtained. Energy Dispersive X-Ray (EDX) analysis (not shown here) confirmed the silicon and oxygen composition.

Figure 3 shows FT-IR spectra obtained from BC, amorphous silica (prepared by TEOS hydrolysis followed by drying at 50 °C) and two representatives BC–silica composites.

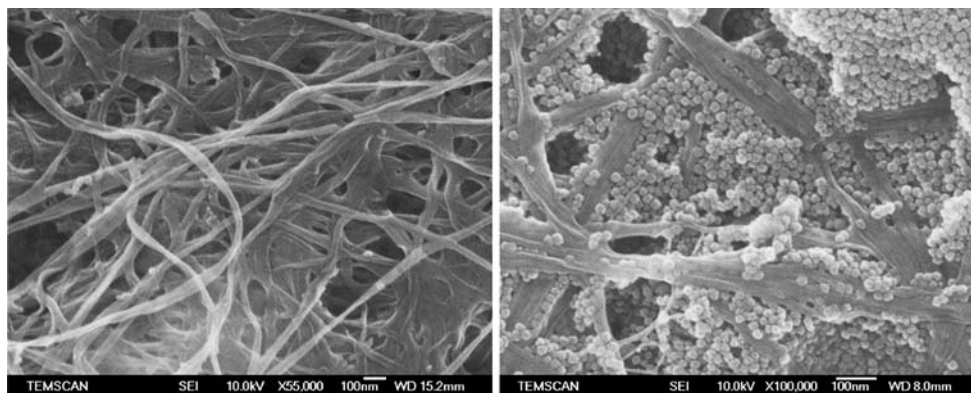


Fig. 1 SEM images of bacterial cellulose membranes (left) and BC-silica (66wt.%) composite (right)

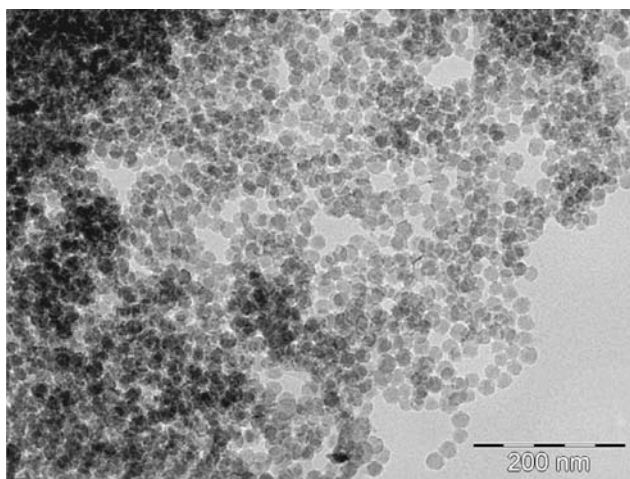


Fig. 2 TEM image of BC-silica 66% composite treated in air at 400 °C

Figure 3a shows the spectrum obtained for BC. The main bands can be assigned to [19]: $3,500\text{ cm}^{-1}$ (OH stretching), $3,246\text{ cm}^{-1}$ (H-bond), $2,908\text{ cm}^{-1}$ (CH stretching of CH_2 and CH_3 groups), $2,700\text{ cm}^{-1}$ - $\nu_s(\text{CH}_2)$, $1,654\text{ cm}^{-1}$ (water OH bending), $1,435\text{ cm}^{-1}$ (CH_2 symmetric bending), $1,370\text{ cm}^{-1}$ (CH bending), $1,160\text{ cm}^{-1}$ (antisymmetric bridge C–O–C stretching), $1,111\text{ cm}^{-1}$ and $1,056\text{ cm}^{-1}$ (skeletal vibrations involving C–O stretching), 895 cm^{-1} (antisymmetric out-of-phase stretching), 667 cm^{-1} , 619 cm^{-1} (OH out-of-phase bending).

Figure 3b shows the spectrum obtained for amorphous silica. The main bands can be assigned to: $3,460\text{ cm}^{-1}$ (water and silanol OH stretching), $1,640\text{ cm}^{-1}$ (water OH bending), $1,110\text{ cm}^{-1}$ (Si–O stretching), 949 cm^{-1} (Si–OH stretching), 804 cm^{-1} (Si–O–Si symmetric stretching), 462 cm^{-1} (Si–O–Si bending).

Spectra presented in Fig. 3c and d can be considered as the result of the convolution of the spectra described here above weighed by the relative quantities of the two components. No important changes could be observed that

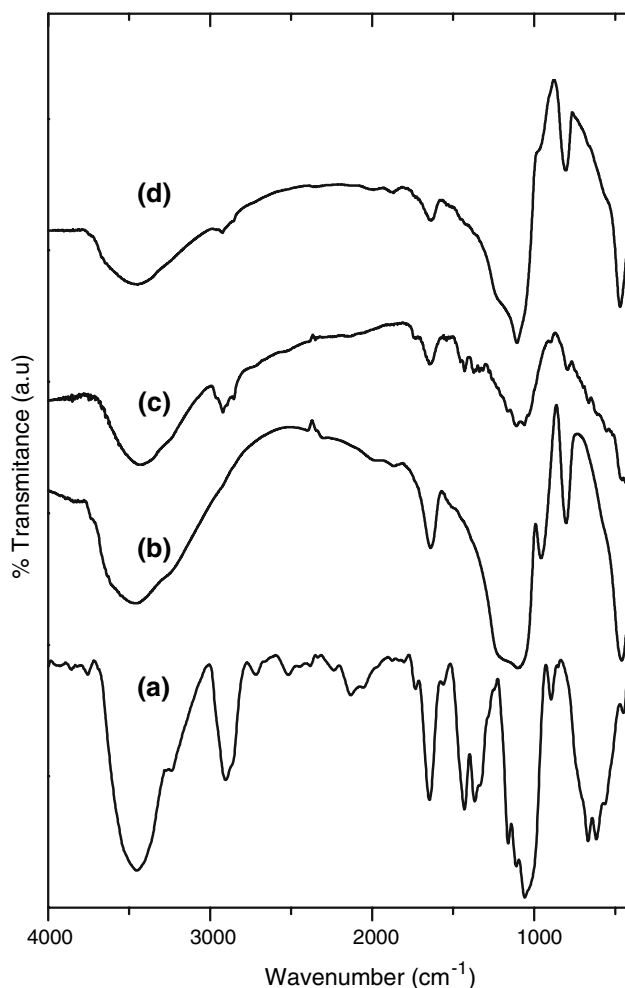


Fig. 3 FTIR spectra: (a) Bacterial cellulose; (b) amorphous silica; (c) cellulose/silica 28%, (d) cellulose/silica 66%

could be related to strong chemical interactions between the cellulose and silica phases. The cellulose H-bond sensitive region above $3,000\text{ cm}^{-1}$ is strongly overlapped with the water molecular vibrations hindering a more detailed analysis.

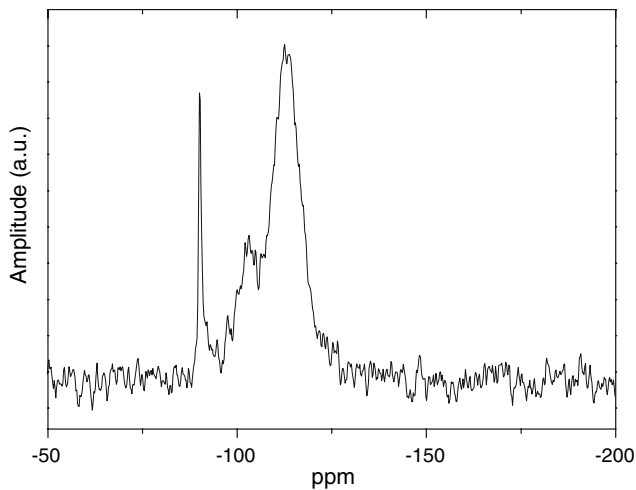


Fig. 4 ^{29}Si MAS NMR spectrum. BC-silica 66% composite

Figure 4 shows a representative solid-state ^{29}Si MAS NMR spectrum obtained for the sample containing 66wt.% silica. Considering the well known different chemical ambient for silicon represented by Q^n notation, the spectrum is dominated by the -113 ppm peak assigned to Q^4 species that is, silicon atoms cross linked by bridging oxygen atoms in a silica network. A high degree of TEOS conversion in condensation reactions is therefore observed. Weaker components are observed at -103 and -89 ppm corresponding to residual Q^3 and Q^2 species, respectively. The condensation degree that can be obtained from the spectrum amounts 92%.

As BC hydrated membranes are soaked in TEOS/Ethanol diffusion of the sol permeates cellulose microfibrils. TEOS hydrolysis/condensation reaction leads to the deposition of silica spheres. It is interesting to compare the results here obtained with other cellulose-silica composites prepared in the literature [15–18]. Since hydrolysis is usually performed in acidic medium silica covering

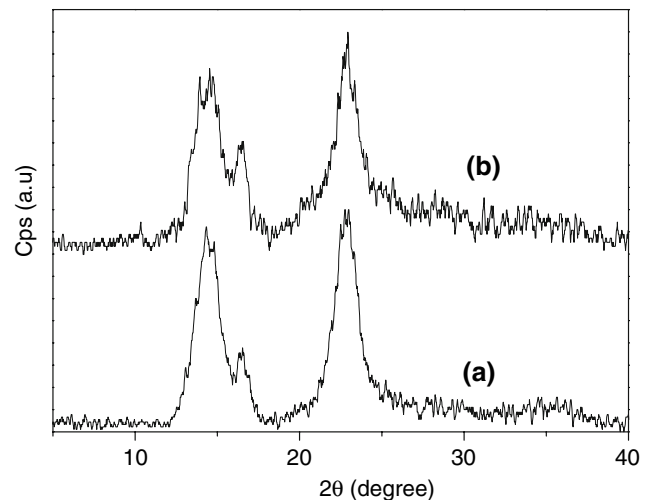


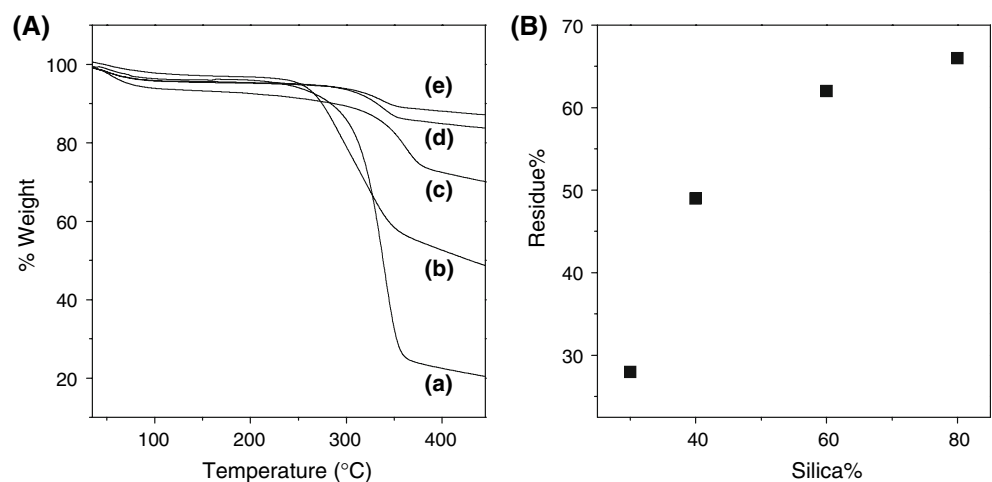
Fig. 5 XRD. (a) BC; (b) BC-silica 66% composite

cellulose fibers is always obtained. The hydrolysis pH employed here is around 5 which is higher than the silica PZC (point of zero charge), therefore favoring silica clustering in spherical morphology [20]. In such way, silica nanospheres can be obtained by silanol self-assembling on cellulose fibrils. When cellulose is removed, 20–30 nm silica spheres could be obtained. Therefore in a way not clear up to now the BC structure seems to control the size and size dispersion of the particles. Further work is needed in order to further understand that property, probably related to condensation reactions involving not only silanol but also cellulose OH groups.

Figure 5 shows XRD patterns for BC and BC-silica 62% composite. Diffraction peaks at 15° and 22.5° are assigned to the cellulose 1α and 1β phases ($100_{1\alpha}$, $110_{1\beta}$ and $010_{1\beta}$ planes at 15° and $110_{1\alpha}$ and $200_{1\beta}$ at 22.5°). Deposited silica nanoparticles seem not to affect the BC crystal structure.

Figure 6A shows TGA curves obtained for BC and hybrids. Two significant weight losses may be observed

Fig. 6 (A) TGA curves: (a) BC; (b) BC-silica 28%; (c) BC-silica 49%; (d) BC-silica 62%; (e) BC-silica 66%. (B) residue % as a function of silica content



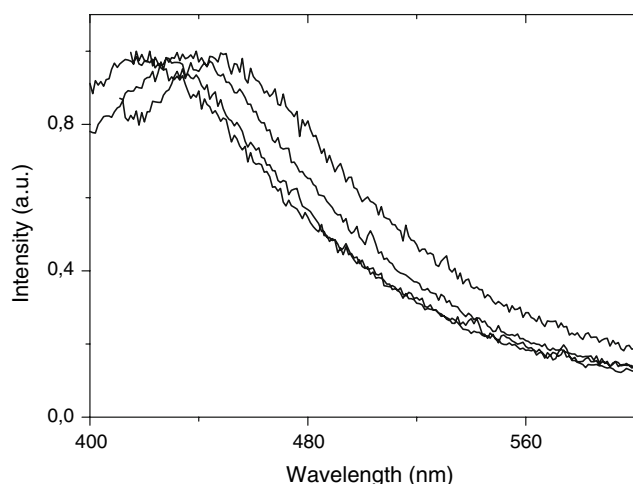


Fig. 7 Room temperature emission spectra. Excitation wavelength (from the left spectrum): 340, 350, 360 and 370 nm

from ambient to 300 °C and from 300 to 400 °C. The first mass loss step is due to membrane dehydration. Physically adsorbed and hydrogen bonded linked water molecules can be lost at that first stage. The second mass loss, corresponding to a broad exothermic peak observed in Differential Thermal Analysis curves (not shown here), can be attributed to BC pyrolysis leading to carbon and silica residue. Figure 6B shows the actual relative content for silica as compared to the nominal concentrations. A saturation point can be observed around 66 wt.% silica.

Figure 7 shows room temperature emission spectra obtained for the BC-silica 66% composite. A broad emission band (bandwidth ~120 nm) is observed for excitation in the UV. Figure also shows that a red shift is observed as the excitation energy decreases. Excitation wavelengths are indicated in the figure.

A broad emission band is observed in other organic-inorganic hybrids and also silica spheres obtained by the so-called Stöber method and treated at temperatures under 500 °C. It can be assigned to electron-hole recombination in oxygen related defects located at the particles surface [5, 21]. The observation of broad band emission from amorphous silica based particles has been claimed before in the literature by several different research groups. However the preparation described here, by using an environmental friendly matrix like BC, opens a new direction in the search for new phosphors. Tuning the emission color is an interesting property observed for these new hybrids with new perspectives of applications in optical devices.

4 Conclusion

BC-silica hybrids were prepared from hydrated BC membranes and TEOS. Macroscopically homogeneous

membranes were obtained containing up to 66 wt.% of 20–30 nm silica spheres that can be recovered by removing cellulose. The new hybrids are stable up to 300 °C and display a broad emission band under UV excitation assigned to oxygen-related defects at the particles surface. Emission color can be tuned by changing the excitation wavelength.

Acknowledgments Authors thank the financial support of the Brazilian agencies CNPq and FAPESP. Also the international cooperation program CAPES (Brazil)-COFECUB (France) contract 471/04 is acknowledged. Dr. C.A. Ribeiro and Dr. S.H. Santagnelli are also acknowledged for the help in TGA and NMR measurements respectively.

References

- Canham LT (1990) *Appl Phys Lett* 57:1046
- Wilson WL, Szajowski PF, Brus LE (1993) *Science* 262:1242
- Pavesi L, Dal Negro L, Mazzoleni C, Franzó G, Priolo F (2000) *Nature* 408:440
- Schimdt H (2006) *J Sol-Gel Sci Technol* 40:115
- Carlos LD, Sá Ferreira RA, de Zéa Bermudez V, Ribeiro SJL (2001) *Adv Funct Mater* 11(2):111
- Klemm D, Heublein B, Fink HP, Bohn A (2005) *Angew Chem Int Ed* 44:3358
- Bielecki S, Krystynowicz A, Turkiewicz M, Kalinowska H (2005) Bacterial cellulose. In: Steinbuechel A, Doi Y (eds) *Biotechnology of biopolymers. From Synthesis to Patents*, Chapter 14. Wiley-VCH, Weinheim, p 381
- Sheridan RL, Morgan JR, Mohamed R (2002) Biomaterials in burn, wound dressings. In: Severian D (ed) *Handbook of polymeric biomaterials*, Chapter 17. Marcel Dekker, New York, p 451
- Czaja WK, Young DJ, Kawecki M, Brown Jr RM (2007) *Biomacromolecules* 8(1):1
- Fontana JD, Souza AM, Fontana CK, Torriani IL, Moreschi JC, Gallotti BJ, Souza SJ, Narcisco GP, Bichara JA, Farah LF (1990) *Appl Biochem Biotechnol* 24/25:253
- Jonas R, Farah LF (1998) *Polym Degrad Stab* 59:101
- Barud HS, Barrios C, Regiani T, Marques RFC, Verelst M, Dexpert-Ghys J, Messaddeq Y, Ribeiro SJL (2007) *Mater Sci Eng C*. doi:10.1016/j.msec.2007.05.001
- Yano S, Iwata K, Kurita K (1998) *Mater Sci Eng C* 6:75
- Tanaka K, Kozuka H (2004) *J Sol-Gel Sci Technol* 32:73
- Dujardin E, Blaseby M, Mann S (2003) *J Mater Chem* 13:696
- Maeda H, Nakajima M, Hagiwara T, Sawaguchi T, Yano S (2006) *J Mater Sci* 41(17):5646
- O’Kelly J, Crockett R, Martin H, Calvert P (1997) *J Sol-Gel Sci Technol* 8:641
- Sequeira S, Evtunguin DV, Portugal I, Esculcas AP (2007) *Mater Sci Eng C* 27:172
- Kondo T, Sawatari C (1996) *Polymer* 37(3):393
- Xu Y, Wu D, Sun Y, Cao H, Yuan H, Deng F (2007) *J Sol-Gel Sci Technol* 42:13
- Carlos LD, Sá Ferreira RA, Pereira RN, Assunção M, de Zéa Bermudez V (2004) *J Phys Chem B* 108:14924